

**Figure 1.** UV-visible absorption of a rigorously oxygen-degassed solution of  $1.79 \times 10^{-4}$  M daunomycin,  $1.79 \times 10^{-3}$  M **6**, and  $2.0 \times 10^{-3}$  M trisma in methanol-*d* solvent at  $25.0 \pm 0.1$  °C as a function of time. Scans were 1 s in duration and occurred every 10 s in the time period 10–130 s.

revealed a fall in the 380- and 608-nm bands with a rise in the 480-nm band. The 420-nm band was assigned to the hydroquinone **4** consistent with absorption in this region for the hydroquinone of 7-deoxydaunomycinone.<sup>12</sup> The bands at 380 and 608 nm were assigned to the tautomer **5**. Daunomycin and 7-deoxydaunomycinone both absorb at 480 nm. The semiquinone **3** is observable by EPR spectroscopy, but its concentration even at maximum is insufficient to produce a significant UV-visible absorption.<sup>13</sup> No additional paramagnetic species were observed. The appearance and breadth of the isosbestic points at 417 and 525 nm are consistent with initial formation of the hydroquinone **4** followed by elimination to the tautomer **5** possibly with some isomerization of tautomer to **2** during the 130-s time period.

The kinetics of formation and destruction of **3** and **5** were observed with  $1.56 \times 10^{-4}$  M **6** and daunomycin and  $2.0 \times 10^{-3}$  M trisma buffer in methanol. At 0.6 °C the EPR signal rose and fell as a function of time with a maximum at 1800 s. The visible absorption signal at 608 nm similarly rose and fell, however, with a maximum at 3000 s clearly distinguishing these two intermediates.

At  $0.86 \times 10^{-4}$  M **6**,  $1.71 \times 10^{-4}$  M **1**, and  $2.0 \times 10^{-3}$  M trisma buffer in methanol in the temperature range 15–25 °C, tautomer concentration as a function of time followed clean consecutive first-order kinetics with the slow steps being bond homolysis of **6** ( $k_1$ ) and tautomerization ( $k_2$ ) as shown in Scheme I. At this concentration of **6**, hydroquinone **4** was not observed because it is produced more slowly, and the isosbestic points at 417 and 525 nm are sharp for both formation and destruction of **5**. The first-order rate constant  $k_2$  ( $0.013 \pm 0.001$  s<sup>-1</sup>) and the molar extinction coefficient for **5** at 620 nm ( $9400 \pm 400$ ) were determined at  $25.0 \pm 0.1$  °C by a nonlinear least-squares fitting of the absorption as a function of time using an independently measured value for  $k_1$ .<sup>9</sup> These experiments and a similar experiment using methanol-*d* solvent gave a  $k_H/k_D = 9.1 \pm 0.5$  and  $\Delta H^\ddagger = 18 \pm 0.5$  kcal/mol and  $\Delta S^\ddagger = -6 \pm 1$  cal/(deg·mol) for the tautomerism.

Kinetic evidence that the semiquinone **3** reacted via reduction to hydroquinone **4** as shown in Scheme I rather than elimination to radical **8** as proposed by others for reaction under somewhat different conditions<sup>5-7</sup> was obtained by EPR spectroscopy. At maximum semiquinone concentration, the rate of formation of **3** equals its rate of destruction. Consistent with Scheme I, the height of the EPR signal for **3** at maximum ( $h_m$ ) is related to the time ( $t_m$ ) at which the maximum is achieved at two different initial concentrations of **6** according to

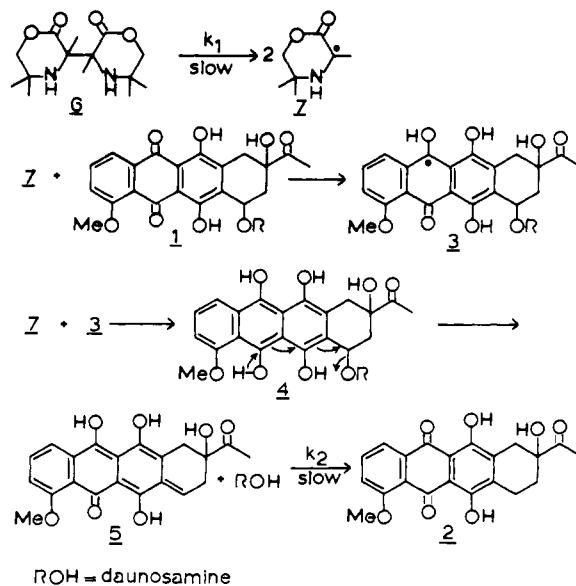
$$h_{m1}/h_{m2} = ([6]_{01}/[6]_{02})e^{k_1(t_{m2}-t_{m1})}$$

(12) The hydroquinone of **2** was generated by anaerobic reaction of **2** with **6**.

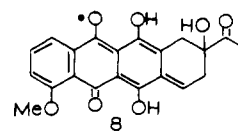
(13) Semiquinone:  $g = 2.0037$ , 2.53 (1:1), 1.98 (1:1), 1.57 (1:1), 1.44 (1:1), 0.92 (1:2:1), 0.50 G (1:2:1).<sup>14</sup>

(14) Lown, J. W.; Chen, H.-H. *Can. J. Chem.* **1981**, *59*, 3212.

**Scheme I**



With  $1.57 \times 10^{-4}$  and  $1.17 \times 10^{-4}$  M initial concentrations of **6**, the observed and calculated values of  $h_{m1}/h_{m2}$  were both  $1.4 \pm 0.1$ . Elimination via **3** to radical **8** does not fit this simple relationship unless reduction of **8** to **5** is slow. If reduction of **8** were slow, **8** would have been observed in the EPR.



In summary we reported here the first experimental evidence for the tautomer **5**, an intermediate resulting from a sequential two-electron reductive glycosidic cleavage of daunomycin. Evidence is thus presented for an intermediate that has been previously proposed as a biologically active form of daunomycin.

### Biosynthesis of Riboflavin. Analysis of Biosynthetically <sup>13</sup>C-Labeled Riboflavin by Double-Quantum and Two-Dimensional NMR

Paul J. Keller, Quang Le Van, and Adelbert Bacher\*

*Lehrstuhl für Organische Chemie und Biochemie  
Technische Universität München  
8046 Garching, West Germany*

John F. Kozlowski and Heinz G. Floss\*\*†

*Department of Medicinal Chemistry and Pharmacognosy  
Purdue University, West Lafayette, Indiana 47907*

Received October 21, 1982

The biosynthesis of riboflavin (**3a**, Scheme I) has been the subject of many recent reports.<sup>1</sup> The terminal step in this pathway is the transfer of a four-carbon unit consisting of carbons 6, 6a, 7, and 7a from one molecule of 6,7-dimethyl-8-ribityllumazine (**2**) to a second molecule of **2**. Diacetyl, acetoin, tetroses, and

\* Address correspondence to Department of Chemistry, The Ohio State University, Columbus, OH 43210.

(1) For reviews see: (a) G. W. E. Plaut, C. M. Smith, and W. L. Alworth, *Ann. Rev. Biochem.*, **43**, 899 (1974); (b) G. M. Brown and J. M. Williamson, *Adv. Enzymol.*, **53**, 345 (1982).

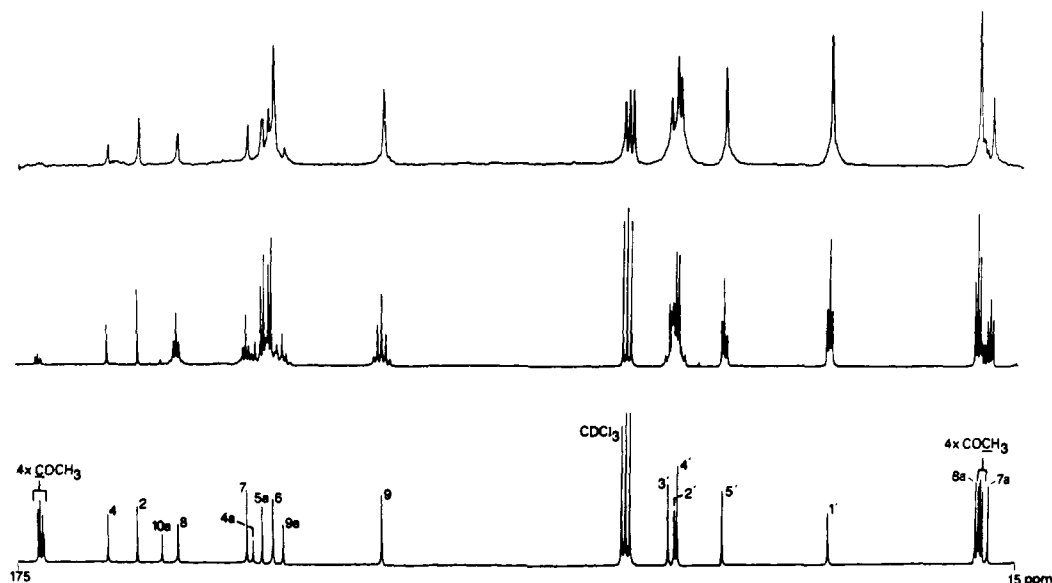


**Figure 1.**  $^1\text{H}$ -decoupled (square-wave modulation) 50.3-MHz  $^{13}\text{C}$  NMR spectra of riboflavin tetraacetate. The bottom trace shows the tetraacetate at natural abundance, and the middle trace shows a similar spectrum of the same compound biosynthesized from D- $[\text{U}-^{13}\text{C}_6]$ glucose. The top trace shows the  $^1\text{H}$  and  $^{13}\text{C}$  broad-band decoupled  $^{13}\text{C}$  NMR spectrum of the labeled sample, obtained by projection of absolute value data from the  $^{13}\text{C}$  homonuclear 2-D-J spectrum. For the 2-D spectrum, the spectral width in the chemical shift dimension was 8 KHz collecting 4K data sets, and in the  $^{13}\text{C}$ - $^{13}\text{C}$  coupling dimension the spectral width was 150 Hz, which was sampled in 128 increments and zero-filled to 256 data points.

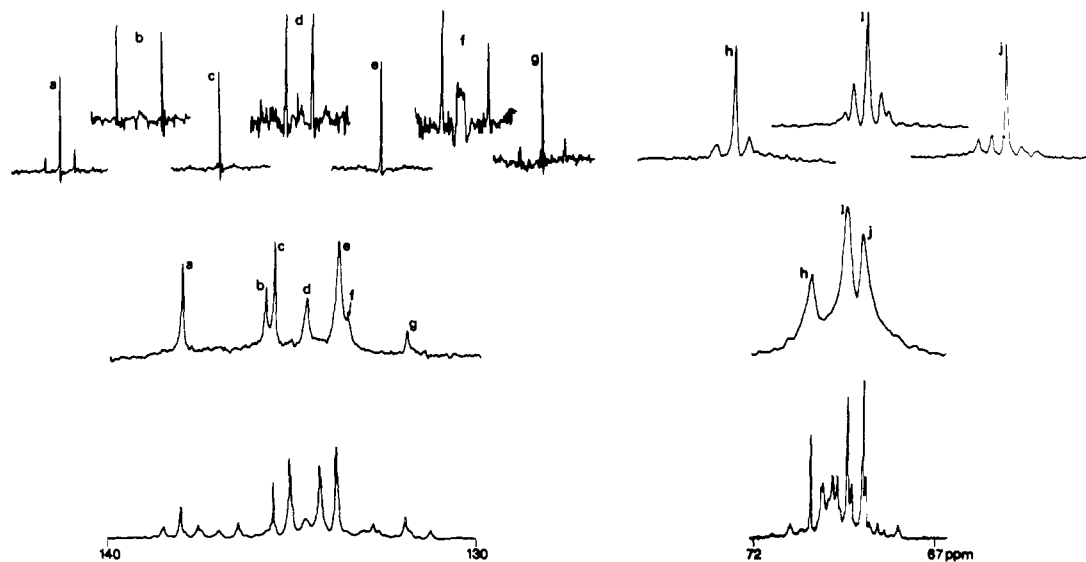


**Figure 2.**  $^{13}\text{C}$  homonuclear 2-D-J spectra of riboflavin tetraacetate from D- $[\text{U}-^{13}\text{C}_6]$ glucose. Shown are the regions containing the ribityl carbons 2', 3', and 4' (right) and the aromatic carbons 4a, 5a, 6, 7, and 9a (left). The top traces are slice plots of the peaks seen in the projections (middle traces). In the aromatic region the slice plots are 150 Hz wide and displayed in the phase-sensitive mode. In the ribityl region the slice plots are 300 Hz wide and are the result of the absolute value summations across 10 Hz in the chemical shift dimension. The one-dimensional spectra of these areas are shown in the bottom traces for comparison. Peak assignments are as follows: a, C-7; b, c, C-5a; d, combination line; e, f, C-6; g, C-9a; h, C-3'; i, C-2'; j, C-4'.

pentoses have been discussed<sup>2</sup> as potential precursors of these four atoms of **2**. Current efforts in our laboratories have involved the incorporation of precursors carrying multiple  $^{13}\text{C}$  labels into riboflavin by the flavinogenic fungus *Ashbya gossypii*. This report concerns the application of recently developed 2-D NMR and double-quantum NMR techniques to analyze the complex  $^{13}\text{C}$  NMR spectra of material from such experiments.

Feeding D- $[\text{U}-^{13}\text{C}_6]$ glucose (0.25 g, 90%  $^{13}\text{C}$ , Merck) to the fungus as previously described<sup>3</sup> gave riboflavin, which was de-

(2) (a) T. W. Goodwin and D. H. Treble, *Biochem. J.*, **70**, 14 (1958); (b) S. N. Ali and U. A. S. Al-Khalidi, *ibid.*, **98**, 182 (1966); (c) K. Bryn and F. C. Stormer, *Biochim. Biophys. Acta*, **428**, 257 (1976); (d) W. L. Alworth, M. F. Dove, and H. N. Baker, *Biochemistry*, **16**, 526 (1977).

(3) A. Bacher, Q. Le Van, M. Bühler, P. J. Keller, V. Eimicke, and H. G. Floss, *J. Am. Chem. Soc.*, **104**, 3754 (1982).

(4) (a) W. P. Aue, J. Karhan, and R. R. Ernst, *J. Chem. Phys.*, **64**, 4226 (1976); (b) R. Freeman and H. D. W. Hill, *ibid.*, **54**, 301 (1971).

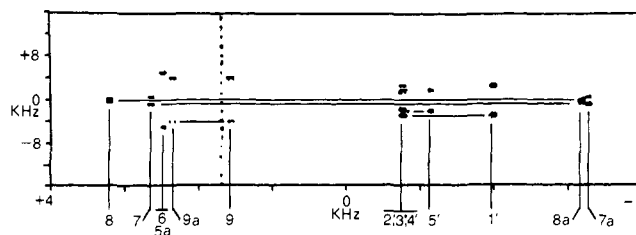
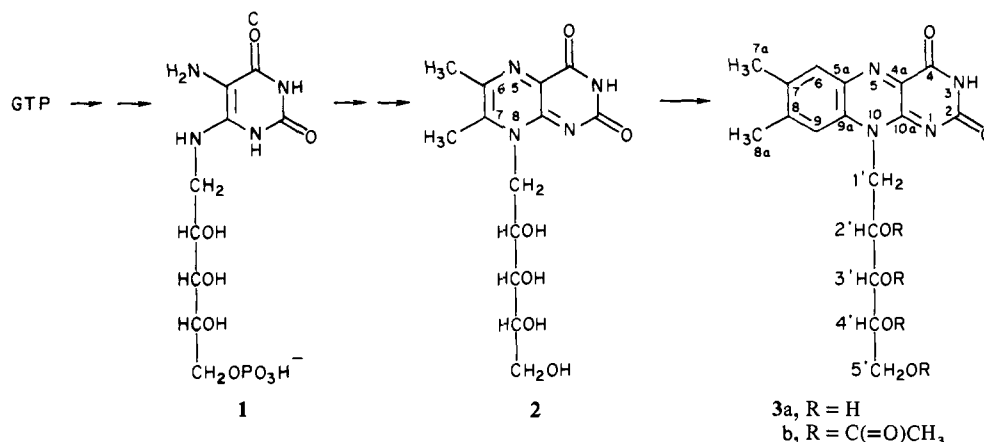


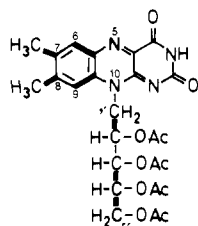
**Figure 3.** 2-D INADEQUATE spectrum of riboflavin tetraacetate from D- $[\text{U}-^{13}\text{C}_6]$ glucose.  $^{13}\text{C}$  chemical shift is along the ordinate and double-quantum frequency is along the abscissa. An artifact is apparent on the left side of the C-9 signal.

rivatized to the tetraacetate (**3b**), 45 mg, overall  $^{13}\text{C}$  enrichment of ca. 15%. The  $^1\text{H}$ -decoupled  $^{13}\text{C}$  NMR spectrum (Varian

Scheme I. Biosynthesis of Riboflavin



Scheme II



XL-200) of this material in  $\text{CDCl}_3$  (Figure 1) exhibits complex multiplets for the ribitol carbons 2', 3', and 4' and for the aromatic carbons 4a, 5a, 6, 7, and 9a. To simplify the spectrum, a  $^{13}\text{C}$ -observe variant of the  $^1\text{H}$  homonuclear 2-D- $J$  spectroscopy method of Aue et al.<sup>4</sup> was implemented with the Varian HOM2DJ program after adjustment of spectral parameters for  $^{13}\text{C}$  observation with  $^1\text{H}$  decoupling. Projection of the data from this  $^{13}\text{C}$  homonuclear 2-D- $J$  spectrum onto the chemical shift axis yielded a  $^{13}\text{C}$  NMR spectrum that was both  $^1\text{H}$  and  $^{13}\text{C}$  "broad-band decoupled" (Figures 1 and 2). The  $^{13}\text{C}$ - $^{13}\text{C}$  coupling information was most conveniently displayed in the form of slice plots. Effects of strong coupling are seen in the aromatic region of the projected spectrum (Figure 2). Symmetrization of AB patterns gives projection signals at the midpoints of the doublets. Peaks b and c represent coupled and uncoupled signals for C-5a, respectively, peaks e and f are the analogous signals for C-6, and peak d is a combination line, the slice plot of which depicts the frequency difference between the inner lines of the AB pattern.

Once the multiplicities had been determined, the nontrivial task of assigning the biochemical connectivities<sup>5</sup> required attention. Bax and co-workers<sup>6</sup> have reported on the use of double-quantum coherence NMR (INADEQUATE) to trace the connectivities of a carbon skeleton through a two-dimensional technique. The 2-D INADEQUATE spectrum of the labeled riboflavin tetraacetate was measured (Figure 3) on the Varian instrument using the program denoted as CCC2D, which yields spectra with a mirror plane on the double-quantum axis. The spectrum clearly shows the incorporation of intact two-carbon units from glucose into the xylene moiety (Scheme II). Thus biochemical connectivities are observed for the following coupled pairs: 7-7a, 8-8a, 9-9a, and 6-5a. The connectivities of the ribitol carbons 1'-2' and 4'-5' were also detected, but the 2'-3' and 3'-4' connectivities were not determined.

A powerful attribute of the 2-D INADEQUATE technique is that the revelation of carbon connectivities often directly leads to signal

assignments. In the present case, if the well-documented<sup>8,9</sup> assignments of carbons 8a and 9 are accepted, then the assignments of 5a, 6, 7, 7a, 8, and 9a are readily apparent. Distinction between carbons 5a and 6 is made on the basis of a directly bonded proton at C-6. 2-D  $^{13}\text{C}$  homonuclear correlation spectroscopy, which was also performed in a manner analogous to the proton experiment,<sup>10</sup> permitted the unambiguous assignments of carbons 2', 3', and 4' based on the couplings of 2' with 1' and 4' with 5'.

On the basis of further  $^{13}\text{C}$  NMR studies at 118 MHz (not reported here), it was found that connectivity between carbons 2' and 3' was only partially retained from glucose, while 3'-4' showed a high degree of connectivity. It is concluded that the majority of the fed glucose did not directly enter the pentose pool by decarboxylation, but rather that there was considerable cycling of glucose through the glycolytic pathway before conversion into a pentose. From the present data it can be concluded that the four carbon atoms of **2** in question arise from the sugar pool as either two two-carbon units or one four-carbon unit but probably not via a 1 + 3 or 1 + 2 + 1 carbon combinations, unless such combinations involve intramolecular rearrangements.

**Acknowledgment.** We thank Dr. Ralph Hurd of Nicolet Instruments, Fremont, CA, for performing the 2-D  $^{13}\text{C}$  homonuclear correlation experiment. This work was supported by the Deutsche Forschungsgemeinschaft (Grant Ba/574/5-6 to A.B.) and by the U.S. Public Health Service (NIH Grant AI 11728 to H.G.F.). H.G.F. and P.J.K. are grateful to the Alexander von Humboldt-Stiftung for a U.S. senior scientist award and a fellowship, respectively.

(8) H. J. Grande, R. Gast, C. G. van Schagen, W. J. H. van Berkel, and F. Müller, *Helv. Chim. Acta*, **60**, 367 (1977).

(9) K. Kawano, N. Ohishi, A. T. Suzuki, Y. Kyogoku, and K. Yagi, *Biochemistry*, **17**, 3854 (1978).

(10) A. Bax, R. Freeman, and G. Morris, *J. Magn. Reson.*, **42**, 169 (1981).

### Mixed-Valence Pyrazine-Bridged Binuclear Complexes of Osmium Amines

Roy H. Magnuson, Peter A. Lay, and Henry Taube\*

Department of Chemistry, Stanford University  
Stanford, California 94305

Received October 12, 1982

We here report the synthesis and properties of the mixed-valence ion  $[(\text{NH}_3)_5\text{Os}(\text{pyz})\text{Os}(\text{NH}_3)_5]^{5+}$  (**I**) which exhibits several striking features, including intense electronic transitions in the

(5) We call "biochemical connectivities" those atomic connectivities that are retained or generated during the biochemical conversion of a precursor to a product.

(6) A. Bax, R. Freeman, and T. A. Frenkiel, *J. Am. Chem. Soc.*, **103**, 2102 (1981).

(7) E. Breitmaier and W. Voelter, *Eur. J. Biochem.*, **31**, 234 (1972).